Structural basis for reversible photoswitching in Dronpa

Martin Andresen*, Andre C. Stiel*, Simon Trowitzsch†, Gert Weber†, Christian Eggeling*, Markus C. Wahl†, Stefan W. Hell*, and Stefan Jakobs*‡

Departments of *NanoBiophotonics and †Cellular Biochemistry/X-Ray Crystallography, Max Planck Institute for Biophysical Chemistry, Am Fassberg 11, 37077 Göttingen, Germany

Edited by Susan S. Taylor, University of California at San Diego, La Jolla, CA, and approved June 25, 2007 (received for review January 23, 2007)

Dronpa is a novel GFP-like fluorescent protein with exceptional light-controlled switching properties. It may be reversibly switched between a fluorescent on-state and a nonfluorescent off-state by irradiation with light. To elucidate the molecular basis of the switching mechanism, we generated reversibly switchable Dronpa protein crystals. Using these crystals we determined the elusive dark-state structure of Dronpa at 1.95-Å resolution. We found that the photoswitching results in a cis–trans isomerization of the chromophore accompanied by complex structural rearrangements of four nearby amino acid residues. Because of this cascade of intramolecular events, the chromophore is exposed to distinct electrostatic surface potentials, which are likely to influence the protonation equilibria at the chromophore. We suggest a comprehensive model for the light-induced switching mechanism, connecting a cascade of structural rearrangements with different protonation states of the chromophore.

fluorescent protein | molecular switch | photochromism | photoisomerization | reversibly switchable fluorescent proteins

Since the cloning of GFP (1) and its first heterologous expression (2, 3), fluorescent proteins (FPs) have revolutionized cell biology. GFP and its variants are the only fully genetically encoded fluorescent probes available. They have enabled noninvasive imaging of reporter gene expression, protein trafficking, and a multitude of biochemical signals in living cells and organisms (for review see refs. 4–6). Variants of the classical FPs are the so-called photoactivatable FPs. These variants may be irreversibly switched by brief and intense illumination from a dark to a bright state or from one color to the other (7, 8).

The recently discovered reversibly switchable FPs (RSFPs) are a further powerful class of FPs for cell biology and beyond. Other than the photoactivatable FPs, RSFPs may be repeatedly and reversibly switched by irradiation between a fluorescent and a nonfluorescent state. Hence they exhibit unique advantages for protein tracking applications, subdiffraction microscopy, and several novel applications that had not been addressable previously (8–13). Dronpa (14) and asFP595 (asulCP, asCP) (15) are the most prominent RSFPs. Like all FPs, they exhibit a GFP-like fold, namely a β-barrel enclosing an α-helix containing the autocatalytically formed chromophore. Because of its low quantum yield, the tetrameric asFP595 is only of limited use for cell biology applications, whereas Dronpa has been successfully used for several protein tracking studies (14, 16, 17). Dronpa is monomeric, displays favorable switching properties, and shows bright fluorescence with a remarkable fluorescence quantum yield of 0.85. Furthermore, several new Dronpa variants with accelerated switching kinetics have been described (18).

Despite its tremendous potential for many applications, little is known about the molecular basis of the switching in Dronpa. Thus far competing models discussing either the light-driven regulation of the chromophoric protonation state by the surrounding protein matrix (19, 20) or postulating a cis–trans isomerization of the chromophore indirectly determining its own protonation state (18) have been suggested.

To unravel this problem we generated Dronpa protein crystals that were reversibly switchable with visible light at ambient conditions. After switching the whole Dronpa crystals we determined its thus far elusive off-state structure by x-ray crystallography. We found that the primary event of the switching is a light-activated cis–trans isomerization of the chromophore together with a cascade of residue rearrangements. Because the electrostatic surface potentials in the chromophoric cis and trans cavities differ substantially, we postulate that the local protein environments in both positions determine different protonation equilibria of the chromophore, which is crucial for its ability to fluoresce.

Results

Reversibly Switchable Dronpa Protein Crystals. Purified Dronpa crystallized into coffin-shaped crystals (in a centered orthorhombic crystal system) that could be reversibly switched with blue (488 ± 5 nm) and UV (405 ± 5 nm) light between a fluorescent and a nonfluorescent form (Fig. 1 *a* and *b*). Repeated switching of whole crystals was accompanied by only ≈2% photobleaching per cycle (Fig. 1*c*). Because the switching of the Dronpa crystals was reversible, we conclude that the crystal lattice did not influence the molecular switching mechanism. To obtain the x-ray structure of Dronpa in the off-state, the crystals were irradiated for 15 min with blue light to transfer the proteins into the nonfluorescent off-state (to ≈5% residual fluorescence of the on-state crystal). These almost nonfluorescent crystals were then immediately flash-frozen in liquid nitrogen and the atomic structure of Dronpa^{Off} was determined.

Comparison of the On- and the Off-State Structure Reveals Complex Intramolecular Rearrangements. We refined the crystal structure of Dronpa^{Off} at 1.95-Å resolution to R_{work} and R_{free} values of 17.4 and 21.6, respectively. The four protomers, which compose one asymmetric unit, exhibit an average ≈0.24 Å rmsd of the C_α atoms; hence, they were considered to be identical (noncrystallographic-symmetry restrains were used only in the first refinement cycles). The overall fold of Dronpa closely resembles that of GFP and related proteins. The chromophore, spontaneously

Author contributions: M.A. and A.C.S. contributed equally to this work; M.A., A.C.S., S.W.H., and S.J. designed research; M.A., A.C.S., S.T., G.W., and M.C.W. performed research; C.E. contributed new reagents/analytic tools; M.A., A.C.S., S.T., G.W., M.C.W., and S.J. analyzed data; and M.A., A.C.S., and S.J. wrote the paper.

The authors declare no conflict of interest.

This article is a PNAS Direct Submission.

Abbreviations: FP, fluorescent protein; RSFP, reversibly switchable FP.

Data deposition: The atomic coordinates and structure factors have been deposited in the Protein Data Bank, www.pdb.org (PDB ID code 2POX).

‡To whom correspondence should be addressed. E-mail: sjakobs@gwdg.de.

This article contains supporting information online at www.pnas.org/cgi/content/full/0700629104/DC1.

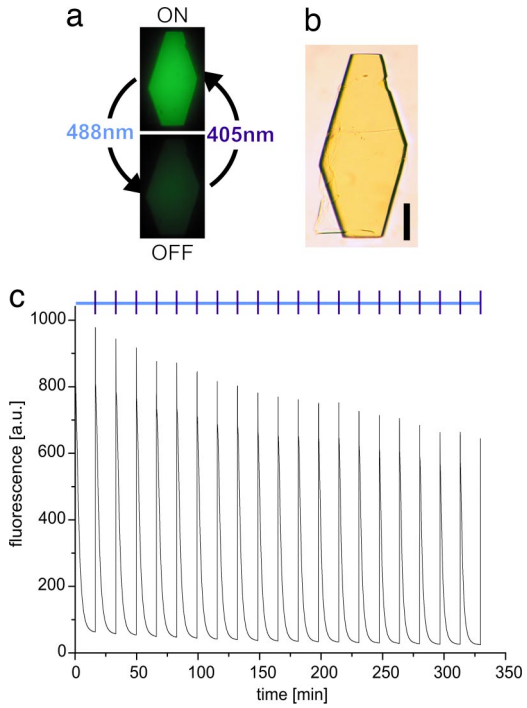

Fig. 1. Reversible photoswitching of Dronpa protein crystals. (*a*) Fluorescence images of a Dronpa crystal in the fluorescent (*Upper*) and nonfluorescent (*Lower*) form. Reversible switching is realized by irradiation with blue (488 ± 5 nm; 0.3 W·cm^{-2}) and UV (405 ± 5 nm; 0.2 W·cm^{-2}) light, respectively. (*b*) Bright-field image of the same crystal. (Scale bar: 50 μm.) (*c*) Fluorescence of the Dronpa protein crystal recorded over 20 switching cycles using the same intensities as in *a*. Repeated excitation sequence, as indicated at the top, was 16.5 min of blue light followed by 4 s of blue and UV light.

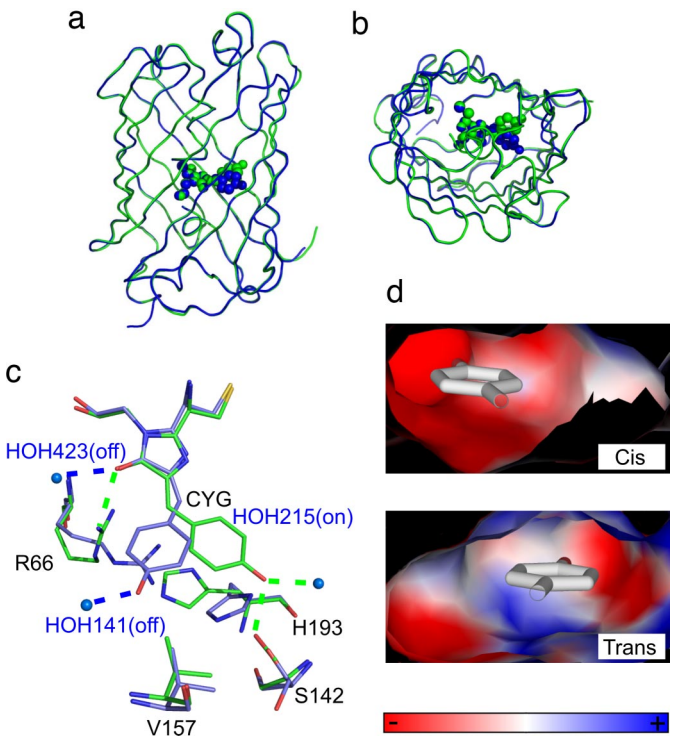

Fig. 2. Comparison of the Dronpa on- and off-structures. (*a* and *b*) Overlay of the on- and the off-structures displayed in two orthogonal views. The chromophore atoms are shown as spheres, and the protein backbones are shown as tubes (on-structure, green; off-structure, blue). (*c*) Detailed comparison of the chromophores and important differences in their vicinities. The chromophores and the residues are shown as sticks, color-coded by atom type (on-state carbon, green; off-state carbon, light blue; oxygen, red; nitrogen, blue; sulfur, yellow). Water molecules are displayed as blue spheres. Hydrogen bonds that disappear in the opposite state are indicated by green and blue dotted lines, respectively. (*d*) Comparison of electrostatic surface potentials [calculated with APBS (22)] of the chromophore cavities around the *p*-hydroxyphenyl ring of the on-state (cis-CYG; *Upper*) and the off-state (trans-CYG; *Lower*). Electrostatic potentials are presented in a color range from red to blue (−10 to +10 *kT*/*e*). Uncharged, hydrophobic surface areas are colorless. Coordinates of the on-structure were taken from ref. 18.

formed from the Cys-62–Tyr-63–Gly-64 (CYG) tripeptide, resides in an α-helical segment, enclosed by an 11-stranded β-barrel, commonly referred to as "β-can" (Fig. 2 *a* and *b*).

In the previously reported fluorescent on-state structures, the chromophore has been shown to adopt a cis-conformation within the β-can (18, 20). In contrast, the Dronpa^{Off} chromophore adopts a trans conformation (Fig. 2*c*). Furthermore, four residues (Arg-66, Ser-142, Val-157, and His-193) that are all located close to the chromophore cavity had changed their positions compared with the on-state structure. With these exceptions, the on- and off-structures were virtually identical (0.22-Å rmsd averaged over the four protomers) (Fig. 2 *a*–*c*).

Upon cis–trans isomerization, the CYG imidazolinone ring almost stays in place, rotating only by 5° (Fig. 2*c*). Therefore, the cis–trans isomerization about the methine bridge connecting the imidazolinone with the the *p*-hydroxyphenyl ring results in a 5.8-Å movement of the apical hydroxyl group of the *p*-hydroxyphenyl ring (Fig. 2*c*). This large movement of the *p*-hydroxyphenyl ring requires translocations of the four aforementioned residues within the β-can. As a result of these structural rearrangements, the side chain of His-193, which forms a pi-stack to the *p*-hydroxyphenyl ring of the on-state CYG, abandons this interaction and is tilted primarily by a 116° rotation around the C_α–C_β bond toward the cis side in the off-state structure (Fig. 2*c*). The His-193 pi-stacking interaction with the *p*-hydroxyphenyl ring is replaced in the off-state by a cation–pi interaction with the side chain of Arg-66. To enable this interaction Arg-66 has changed its on-state position close to the imidazolinone ring to a position beneath the chromophore, resulting in an elongated conformation of the side chain. Further, in the off-state structure, Ser-142 and Val-157 move by 0.5 and 1.0 Å, respectively, enlarging the chromophore cavity. Finally, the side chain of Ser-142, which is stabilized by a hydrogen bond to the hydroxyl group of the *p*-hydroxyphenyl ring in the on-state, has abandoned this bond in the off-state. Instead, it adopts two alternative structures because of a lack of attachment. Because structural information is available only on the on- and the off-state structure, we cannot discriminate whether the observed rearrangements occur simultaneously or sequentially.

Differences Between the On- and the Off-State Structures Point to a Connection Between Structure and Fluorescence. Structurally, the trans(off-state)-CYG is characterized by a distinct torsion and a less rigid attachment to the protein matrix. Whereas the on-state chromophore is only slightly noncoplanar (≈15°), the imidazolinone and the *p*-hydroxyphenyl rings are out of planarity in the off-state by ≈30° (averaged across the four protomers of the asymmetric unit). The cis(on-state)-CYG is very well stabilized, participating in 10 hydrogen bonds to nearby residues, three water-mediated hydrogen bonds, and numerous van der Waals interactions [supporting information (SI) Fig. 5] (18, 20). The nonfluorescent trans-CYG is less strongly attached, exhibiting eight hydrogen bonds and four water-mediated hydrogen bonds (Fig. 2*c* and SI Fig. 6). Most notably, the hydrogen bond to Ser-142, the only hydrogen bond to an amino acid residue

stabilizing the *p*-hydroxyphenyl ring, is absent in the off-state structure. Also, the pi-stacking interaction of the imidazolinone ring with His-193 is replaced by an interaction with Arg-66 in the off-state. We conclude that the cis-chromophore, because of its higher planarity and more rigid attachment to the protein matrix, favors fluorescence as compared with the trans-chromophore.

The conformational changes of the chromophore itself introduced by the cis–trans isomerization may have some influence on its protonation state (21). However, the major influence on the chromophoric protonation state is likely exerted by the local cavity environment. Therefore, we next compared the electrostatic surface potential [calculated with APBS software omitting the chromophore (22)] of the chromophore cavity in the on-state with that of the off-state (Fig. 2*d*). We find that the cavity section enclosing the tyrosyl ring of the cis-(on-state-)chromophore exhibits a predominantly negative surface potential. The corresponding cavity section of the trans-(off-state-)chromophore is strikingly distinct; it has a surface potential ranging from neutral to positive. The standard parameters used for the calculations may not be fully adequate for the special situation of the chromophore cavity. Furthermore, the interdependence between the surface potential and the chromophore protonation is likely to be very complex, rendering it difficult to predict the protonation state of the chromophore from the calculated surface potentials. However, the calculations demonstrate that the cis- and the trans-cavity differ substantially, most likely determining different protonation equilibria of the chromophore.

We conclude that upon a cis–trans isomerization the chromophore faces different local environments with distinct surface potentials. These differences determine that the fluorescent on-state CYG is deprotonated, whereas the nonfluorescent off-state CYG is in its protonated (neutral) state. In conjunction with the differences in chromophore stabilization and planarity, these changes ultimately determine the ability of Dronpa to fluoresce.

Discussion

Cascade of Residue Relocations. Based on crystal structures of the on-state Dronpa, two conflicting models for photoswitching of this protein have been proposed previously. One model suggested that photoswitching of Dronpa depends on subtle conformational changes within and around the environment of the chromophore that promote proton transfer along an intricate polar network (20). The second model proposed a cis–trans isomerization of the chromophore accompanied by several residue rearrangements in the chromophore environment as structural key events of the switching process (18). The data presented in this study strongly support the second model.

This finding is in line with molecular dynamics simulations on the GFP variant E^2GFP, which suggested a cis–trans photoisomerization of the chromophore (12). A light-induced cis–trans isomerization as a key element in the switching process has also been demonstrated for asFP595 (23). Hence the light-induced cis–trans isomerization of the chromophore appears to be a general event in switching of RSFPs.

Switching in Dronpa is exceptional, because it does involve in addition to the cis–trans isomerization considerable rearrangements of internal side chains. Based on the assumption that the light-induced movement of the chromophore induces all subsequent intramolecular events in Dronpa, a model describing the sequential flow of structural rearrangements culminating in the conversion of the $Dronpa^{On}$ into the $Dronpa^{Off}$ structure and vice versa can be envisioned (Fig. 3). After the absorption of a blue photon the excited on-state cis chromophore either fluoresces or it dissipates its energy by isomerizing toward the trans position (a, see Fig. 3); simultaneously with the cis–trans isomerization, the pi-stacking interaction between His-193 and the CYG *p*-hydroxyphenyl ring as well as the hydrogen bond between the tyrosyl oxygen and Ser-142 break (a). Still, the completion of the CYG cis–trans isomerization is sterically opposed by Val-157 and Arg-66. Hence Val-157 needs to move outward, making room for the trans chromophore (b). Simultaneously, the Arg-66 residue changes its position, forming a cation–pi interaction with the *p*-hydroxyphenyl ring, replacing the previous pi-stacking interaction with His-193 (c). Now Arg-66 occupies a position under the chromophore and therefore His-193 changes its conformation by a rotation of the side chain (d). This movement requires Ser-142 to free space for the side chain of His-193 (e). Because Ser-142 no longer forms a stabilizing hydrogen bond to the tyrosyl oxygen, it is found in two alternative conformations in the off-state structure.

The UV light-driven back-transition from the nonfluorescent trans-state to the fluorescent cis state may be regarded as the reverse of the sequential flow of intramolecular events outlined above. Because of the UV light-driven isomerization of the chromophore, the His-193 residue is required to change its position, finally forming a pi-stack with the *p*-hydroxyphenyl ring. Therefore, Arg-66 changes its localization and allows Val-157 to move closer toward the chromophore cavity. Simultaneously, Ser-142 forms a hydrogen bond with the tyrosyl oxygen and adopts a defined spatial position, restoring the fluorescent cis chromophore.

Dronpa is almost bistable, with the nonfluorescent state exhibiting a half-life of ≈14 h (18). The energy barrier governing this bistability appears to be determined by the energy required for the cis–trans isomerization and the residue rearrangements. Because we addressed in this study the ground states we have only limited information on the residues that transiently interact with the moving chromophore. Examples for such interfering residues are Val-157 and Met-159, because their exchange against smaller residues increases the rate of photoswitching to the dark state and simultaneously reduces the half-life of the dark state (18). Hence, exchange of these residues appears to influence the energy barrier for switching. It is noteworthy that in Dronpa switching requires high-energy UV or blue photons, respectively, whereas in asFP595, for which no residue rearrangements have been observed, green and blue photons are sufficient. It will require further studies to determine the influence of the residue rearrangements on the energy landscape of light-induced switching in Dronpa.

A Model for Light-Driven Switching of Fluorescence. Irrespective of the exact succession of intramolecular events discussed above, which has to be experimentally verified, three characteristics of Dronpa appear to be essential for the reversible switching process: (*i*) The local chromophoric cavity environments are distinct in the cis and trans states. (*ii*) Because of the influence of the different cavity environments, the cis-state CYG is predominantly deprotonated; the trans-state CYG is predominantly in a protonated (neutral) state. (*iii*) The deprotonated CYG is fluorescent and absorbs blue light, whereas the protonated CYG is nonfluorescent and absorbs UV light (14, 19).

We propose that these properties may be integrated in a, necessarily simplified, model for the switching process of Dronpa (Fig. 4). At equilibrium, the CYG adopts a cis (on-state) conformation (18, 20). Because of the cis cavity, the CYG is predominantly deprotonated and hence fluorescent, exhibiting a strong absorption peak at 503 nm (blue light), but negligible absorption at 390 nm (UV light). Hence blue light is efficiently absorbed and may induce a cis-to-trans isomerization of the chromophore. Subsequently, in the trans (off-) state, the chromophore is predominantly protonated due to the influence of the cavity. The protonated CYG is nonfluorescent; its ability to fluoresce is further suppressed by its strong torsion, a configuration well known to oppose fluorescence (24) as well as by its loose attachment to the protein matrix, likely opening further

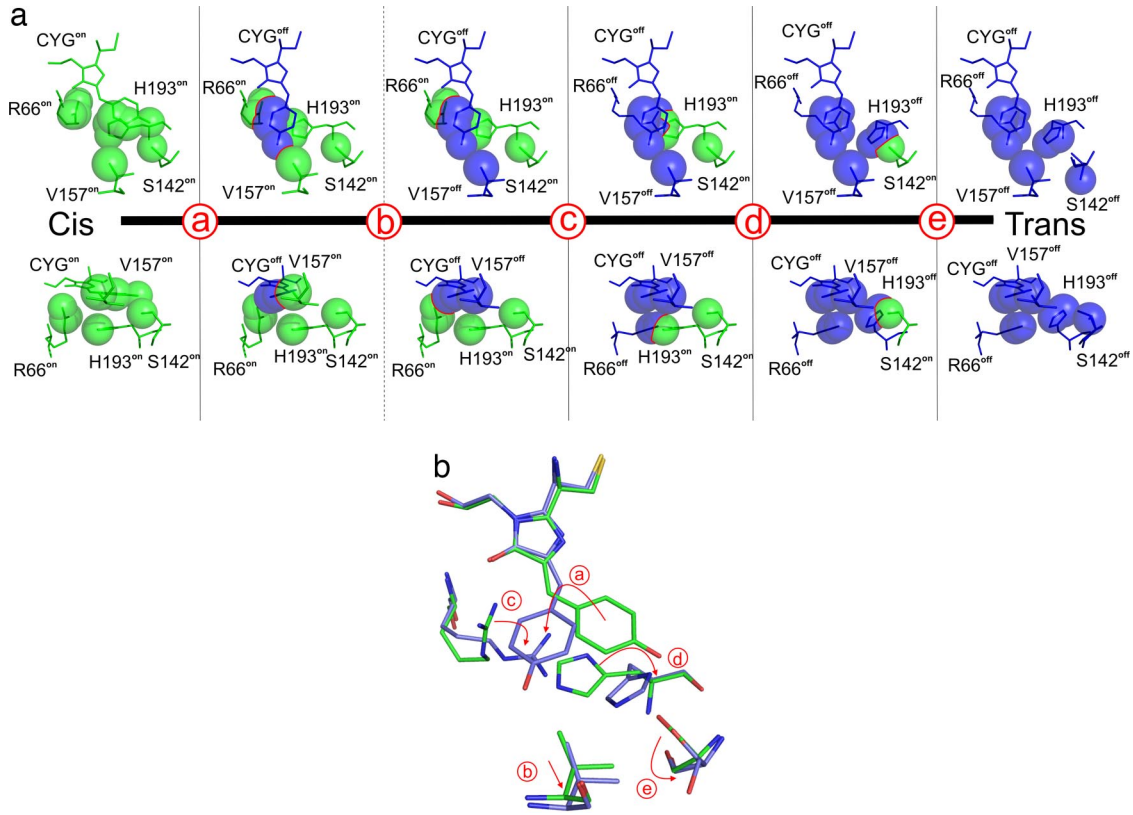

Fig. 3. Model for a cascade of residue rearrangements upon light-induced cis–trans isomerzation. (*a*) The proposed flow of residue arrangements initiated by the cis-to-trans isomerization of the chromophore is outlined. The lower view is tilted by 60° compared with the top view. Residues, as determined in the on- and off-state x-ray structures, are displayed in green and blue, respectively. Only van der Waals radii of atoms that exhibit a potential overlap during the course of the rearrangements are indicated by spheres. Potential spatial clashes evoked by residue rearrangements are indicated by red lines between van der Waals spheres. (*b*) Overview of the chromophore and important surrounding residues in the on- and the off-state structures as in Fig. 2*c*. The localizations of the residue movements as indicated in *a* are highlighted.

channels for a nonradiative decay of energy. The protonation of the trans (off-state)-CYG also changes the absorption spectrum of the protein, resulting in a strong absorption peak for UV light but almost none for blue light. Therefore, although blue light does facilitate the cis-to-trans isomerization, induction of the reverse trans-to-cis isomerization is marginal. Hence the protonation-dependent changes of the absorption spectra of the CYG are crucial for the switching process. Finally, irradiation of the protonated trans (off-state) CYG with UV light induces a trans-to-cis isomerization. In the cis position, the CYG is predominantly deprotonated and the protein is back in the initial on-state.

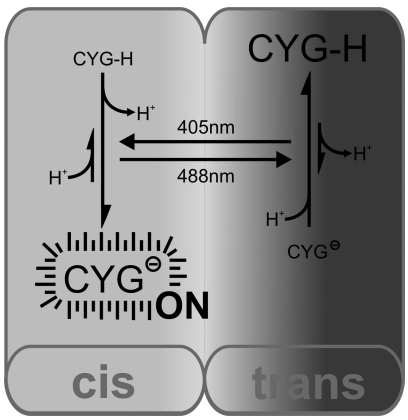

Fig. 4. Model for reversible photoswitching in Dronpa, connecting light-induced intramolecular changes with different protonation states of the chromophore.

Although this model explains numerous properties of Dronpa, it is necessarily simplified. Next to the anionic and neutral forms of the chromophore, a zwitterionic form may also exist, as has been proposed for asFP595 (21). Hence a shift of the protonation equilibrium might also occur at the imine nitrogen N^1 of the imidazolinone ring. In addition, recent studies indicated further photophysical states of Dronpa, which are not addressable by x-ray structural analysis (19, 25), and we expect further photophysical states to be revealed in future studies.

Conclusion and Perspective

We have presented a comprehensive structural model for the molecular mechanism of reversible switching in Dronpa. It connects the light-activated cis–trans isomerization of the chromophore and the accompanying cascade of intramolecular residue rearrangements with different protonation states of the chromophore that are crucial for the absorption and fluorescence properties of this protein. The model outlined here likely describes a general mechanism for light-controlled switching in RSFPs.

Materials and Methods

Protein Production and Purification. The expression plasmid pRSETb-Dronpa was a generous gift from A. Miyawaki (Riken Brain Science Institute, Tokyo, Japan). Proteins were expressed

and purified as described (18). The purified protein was concentrated to ≈23 mg/ml by ultrafiltration and taken up in 20 mM Tris·HCl and 120 mM NaCl (pH 7.5) for crystallization.

Crystallographic Analysis. Dronpa was crystallized as described (18). To switch whole Dronpa protein crystals into the off-state, the crystals were irradiated in the crystallization solution with blue light (488/10 nm; ≈0.3 W·cm^{-2}) until the fluorescence decreased to ≈5% of the initial value. After switching, care was taken to handle the crystals under red light illumination. Immediately after switching, the crystals were transferred into perfluoropolyether and flash-frozen in liquid nitrogen. Diffraction data were collected at the PXII beamline of the Swiss Light Source (Villigen, Switzerland) at 100 K, using a MarResearch CCD detector and processed with the HKL package (26) (SI Table 1).

Structure solution and refinement were performed similarly to the procedures outlined for the on-state structure of Dronpa (18). Briefly, the off-state structure was solved by molecular replacement with MOLREP (27) using the structure coordinates of Dronpa in the on-state (Protein Data Bank entry 2IOV) (18) but omitting the chromophore. After it became clear that residues in the vicinity of the chromophore had changed conformations upon switching, the structure solution was repeated with a model, in which Arg-66, Ser-142, Val-157, and His-193 in addition to the chromophore had been omitted, to reduce model bias. The partial structure was refined automatically with Refmac5 (28) and by manual model building with COOT (29). After convergence, the omitted residues and the chromophore were placed manually into vacant patches of the $2F_o - F_c$ and $F_o - F_c$ electron densities. The water structure was automatically built with Arp/wArp (30) and completed manually. During the entire refinement procedure, 5% of randomly selected reflections were set aside for monitoring of the R_{free} factor (SI Table 1).

Optical Switching. Photoswitching experiments were performed by using a custom-built computer-controlled fluorescence microscope (Leica, Benzheim, Germany) equipped with a ×40N.A. 0.6 air objective lens and two 100-W Hg lamps. For reversible switching, blue light (488/10-nm excitation filter; ≈0.3 W·cm^{-2}) and UV light (405/10-nm excitation filter; ≈0.2 W·cm^{-2}) were used. Fluorescence intensities were recorded with a photomultiplier tube (HR9306-0; Hamamatsu, Hamamatsu City, Japan) using a 500-nm longpass detection filter (HQ 500 LP; AHF Analysentechnik, Tübingen, Germany). For reversible switching, protein crystals in crystallization solution were irradiated consecutively with blue light (inducing the on-to-off transition) and with blue light together with UV light (inducing the off-to-on transition).

Analysis of Crystal Structures. Electrostatic potential maps of the chromophore cavities were calculated with APBS software (22) and visualized with the PyMol program (www.pymol.org). Surface potentials were calculated by omitting the chromophore.

Schematic representation of the hydrogen bonds between the chromophore and the surrounding residues (see SI Fig. 5) were calculated with HBPLUS/LIGPLOT software (31). Calculations were based on the A and the D protomer of the on-state (Protein Data Bank entry 2I0V) and the off-state structure, respectively.

We thank Prof. A. Miyawaki for providing the plasmid pRSETb-Dronpa, S. Löbermann for excellent technical assistance, and J. Jethwa for carefully reading the manuscript.

1. Prasher DC, Eckenrode VK, Ward WW, Prendergast FG, Cormier MJ (1992) *Gene* 111:229–233.
2. Chalfie M, Tu Y, Euskirchen G, Ward WW, Prasher DC (1994) *Science* 263:802–805.
3. Inouye S, Tsuji FI (1994) *FEBS Lett* 341:277–280.
4. Tsien RY (1998) *Annu Rev Biochem* 67:509–544.
5. Chudakov DM, Lukyanov S, Lukyanov KA (2005) *Trends Biotechnol* 23:605–613.
6. Giepmans BN, Adams SR, Ellisman MH, Tsien RY (2006) *Science* 312:217–224.
7. Lippincott-Schwartz J, Altan-Bonnet N, Patterson GH (2003) *Nat Cell Biol* 5:S7–S14.
8. Lukyanov KA, Chudakov DM, Lukyanov S, Verkhusha VV (2005) *Nat Rev Mol Cell Biol* 6:885–891.
9. Miyawaki A (2004) *Nat Biotechnol* 22:1374–1376.
10. Sauer M (2005) *Proc Natl Acad Sci USA* 102:9433–9434.
11. Jakobs S (2006) *Biochim Biophys Acta* 1763:561–575.
12. Nifosi R, Tozzini V (2006) *Chem Phys* 323:358–368.
13. Remington SJ (2006) *Curr Opin Struct Biol* 16:714–721.
14. Ando R, Mizuno H, Miyawaki A (2004) *Science* 306:1370–1373.
15. Lukyanov KA, Fradkov AF, Gurskaya NG, Matz MV, Labas YA, Savitsky AP, Markelov ML, Zaraisky AG, Zhao XN, Fang Y, *et al.* (2000) *J Biol Chem* 275:25879–25882.
16. Aramaki S, Hatta K (2006) *Dev Dyn* 235:2192–2199.
17. Fujioka A, Terai K, Itoh RE, Aoki K, Nakamura T, Kuroda S, Nishida E, Matsuda M (2006) *J Biol Chem* 281:8917–8926.
18. Stiel AC, Trowitzsch S, Weber G, Andresen M, Eggeling C, Hell SW, Jakobs S, Wahl MC (2007) *Biochem J* 402:35–42.
19. Habuchi S, Dedecker P, Hotta J, Flors C, Ando R, Mizuno H, Miyawaki A, Hofkens J (2006) *Photochem Photobiol Sci* 5:567–576.
20. Wilmann PG, Turcic K, Battad JM, Wilce MC, Devenish RJ, Prescott M, Rossjohn J (2006) *J Mol Biol* 364:213–224.
21. Schäfer LV, Groenhof G, Klingen AR, Ullmann GM, Boggio-Pasqua M, Robb MA, Grubmüller H (2007) *Angew Chem Int Ed* 46:530–536.
22. Baker NA, Sept D, Joseph S, Holst MJ, McCammon JA (2001) *Proc Natl Acad Sci USA* 98:10037–10041.
23. Andresen M, Wahl MC, Stiel AC, Gräter F, Schäfer LV, Trowitzsch S, Weber G, Eggeling C, Grubmüller H, Hell SW, Jakobs S (2005) *Proc Natl Acad Sci USA* 102:13070–13074.
24. Patnaik SS, Trohalaki S, Pachter R (2004) *Biopolymers* 75:441–452.
25. Habuchi S, Ando R, Dedecker P, Verheijen W, Mizuno H, Miyawaki A, Hofkens J (2005) *Proc Natl Acad Sci USA* 102:9511–9516.
26. Otwinowski Z, Minor W (1997) *Methods Enzymol* 276:307–326.
27. Vagin AA, Isupov MN (2001) *Acta Crystallogr D* 57:1451–1456.
28. Murshudov GN, Vagin AA, Dodson EJ (1997) *Acta Crystallogr D* 53:240–255.
29. Emsley P, Cowtan K (2004) *Acta Crystallogr D* 60:2126–2132.
30. Morris RJ, Perrakis A, Lamzin VS (2003) *Methods Enzymol* 374:229–244.
31. Wallace AC, Laskowski RA, Thornton JM (1995) *Protein Eng* 8:127–134.